Journal of Magnetic Resonance 212 (2011) 455–459

Contents lists available at SciVerse ScienceDirect

Journal of Magnetic Resonance

journal homepage: www.elsevier.com/locate/jmr

Communication

Rotor-synchronized dipolar-filter sequence at fast MAS in solid-state NMR

Qing-Hua Liu [a], Chao Ma [c], Bing-Wen Hu [a,*], Qun Chen [a,*], Julien Trebosc [b], Olivier Lafon [b], Jean-Paul Amoureux [b,*]

[a] Physics Department & Shanghai Key Laboratory of Magnetic Resonance, East China Normal University, Shanghai 200062, China
[b] UCCS, University Lille North of France, Villeneuve d'Ascq 59650, France
[c] Department of Radiology, Changhai Hospital, Second Military Medical University, Shanghai 200433, China

ARTICLE INFO

Article history:
Received 13 May 2011
Revised 21 July 2011
Available online 10 August 2011

Keywords:
Solid-state NMR
Dipolar-filter
Ultra-fast MAS
Polymers
Homo-nuclear dipolar interactions

ABSTRACT

Dipolar filters are of considerable importance for eliminating the ^{1}H NMR signal of the rigid components of heterogeneous compounds while selecting the signal of their mobile parts. On the basis of such filters, structural and dynamical information of these compounds can often be acquired through further manipulations (*e.g.* spin diffusion) on the spin systems. To overcome the destructive interferences between the magic angle spinning (MAS) speed and the cycle-time of the widely-used Rotor-Asynchronized Dipolar Filter (RADF) sequence, we introduce a new method called Rotor-Synchronized Dipolar Filter (RSDF). This communication shows that this sequence does not present any interference with the spinning speed and is more compatible than RADF with high MAS frequencies ($\nu_R > 12$ kHz). This new pulse sequence will potentially contribute to future researches on heterogeneous materials, such as multiphase polymer and membrane systems.

1. Introduction

Heterogeneous materials, such as multiphase polymers and membrane systems, are often constituted by two or even more components, with different mobility or rigidity in the different phases. In nuclear magnetic resonance (NMR), rigid segments lead to uninformative broad peaks that often obscure the informative narrow peaks of the mobile segments in the ^{1}H spectra. There is thus a significant interest of eliminating the rigid segment signals, while only keeping those related to the mobile parts. Moreover, elimination of the rigid segment signals can lead to polarization gradients between two different segments, which combined with spin diffusion sequences allow (i) to quantify domain sizes in phase separated polymers [1], and (ii) to probe the chain inter-penetration or miscibility in various polymer blends [2].

The Goldman–Shen sequence [3], or a simple ^{1}H dipolar-echo sequence [4], can be used for this purpose. Both methods can eliminate the signals of rigid segments and partially keep those of mobile segments owing to the fact the transverse dephasing time of the mobile segments is much longer than that of the rigid parts. However, both sequences suffer from the fact that the magnetization of the soft phase is decreased significantly by the filtering process. Another disadvantage of the Goldman–Shen sequence is the distortion of the ^{1}H time domain signal at very short spin diffusion times [5].

These limitations are circumvented by the magic and polarization echo (MAPE) [6], and the Rotor-Asynchronous Dipolar-Filter (RADF) sequence, proposed by Egger et al. in 1992 (Fig. 1a) [7–12]. The RADF sequence (Fig. 1a), which was initially designed as a homo-nuclear decoupling method for static samples, consists of a basic cycle of 12 $\pi/2$-pulses of length τ_p, all separated by a delay τ, and repeated for M times. The period of the RADF sequence is thus: $\tau_{RADF} = 12(\tau + \tau_p)$. The phases of the 12 $\pi/2$-pulses in the basic RADF element can be written explicitly as (x, $-y$, x, x, $-y$, x, $-x$, y, $-x$, $-x$, y, $-x$). The RADF pulse sequence is designed to suppress under static condition all spin interaction terms (homo- and hetero-nuclear dipolar, isotropic and anisotropic chemical shift and J-coupling) for the irradiated isotope in the first-order Average Hamiltonian (AH). In the following, the irradiated isotopes are protons and the largest spin interactions are the ^{1}H–^{1}H dipolar couplings. Under static condition, if the magnitudes of ^{1}H–^{1}H dipolar couplings for some ^{1}H sites are small compared to the frequency $1/\tau_{RADF}$, the AH may be approximated by its first-order term and the RADF sequence eliminates all spin interactions for these ^{1}H sites. On the contrary, in the case of ^{1}H sites experiencing dipolar interactions larger than $1/\tau_{RADF}$, the truncation of Average Hamiltonian to its first-order term is not valid and the ^{1}H–^{1}H dipolar interactions are not suppressed by the RADF sequence, which leads to signal dephasing and hence attenuation at a long RADF time. This signal decrease, related to a coherent process, is moreover enhanced by an incoherent process since the ^{1}H sites experiencing

* Corresponding authors.
E-mail addresses: bwhu@phy.ecnu.edu.cn (B.-W. Hu), qchen@ecnu.du.cn (Q. Chen), jean-paul.amoureux@univ-lille1.fr (J.-P. Amoureux).

1090-7807/$ - see front matter © 2011 Elsevier Inc. All rights reserved.
doi:10.1016/j.jmr.2011.07.025

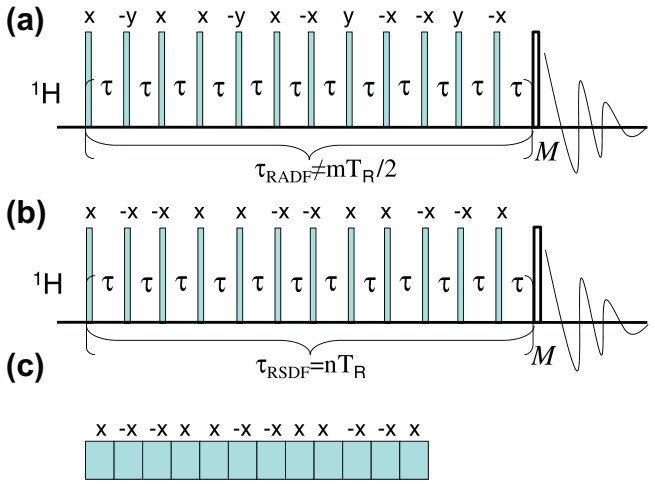

Fig. 1. (a) Rotor-Asynchronous Dipolar-Filter (RADF) sequence [7]. (b) Rotor-Synchronous Dipolar-Filter (RSDF) sequence. (c) Basic cycle of $C6_n^3$ $(x, -x)$ sequence lasting nT_R. All pulses correspond to a 90° flip-angle in (a–c).

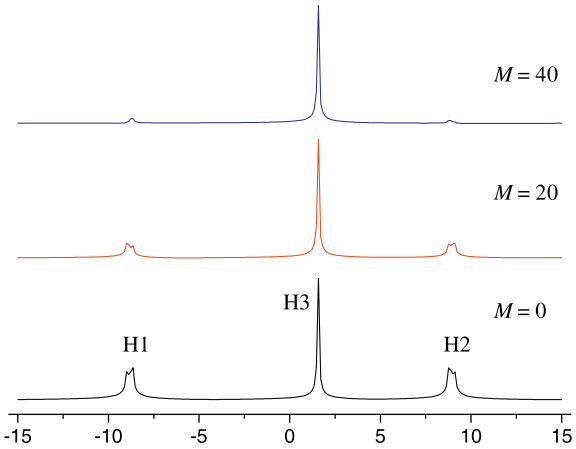

Fig. 2. Simulated ^{1}H spectra of a model spin system obtained using RSDF sequence, shown in Fig. 1b at $B_0 = 14.4$ T and $\nu_R = 30$ kHz, with $n = 4$. The pulse and window lengths are $\tau = 9.11$ μs and $\tau_p = 2$ μs, respectively. The M value is indicated on the figure, and corresponds to $\tau_{tot} = 10.7$ and 21.3 ms, for $M = 20$ and 40, respectively.

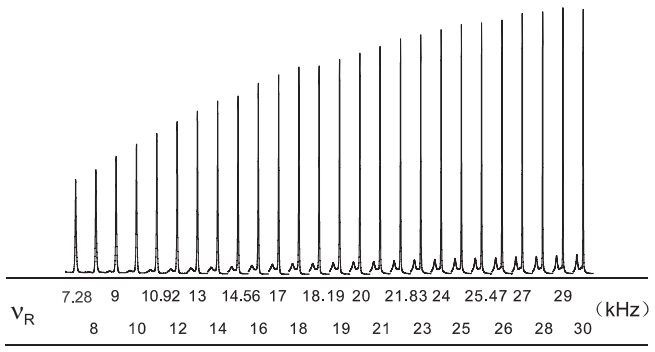

Fig. 3. ^{1}H MAS NMR spectra of the 1/1 GA mixture at $B_0 = 14.4$ T, versus spinning speed ν_R. The shielded narrow peak corresponds to the CH and CH_2 protons of adamantane and the unshielded broad peaks correspond to the NH_3 and CH_2 protons of α-glycine.

weak dipolar interactions are more mobile and they display longer coherence lifetimes than the ^{1}H sites experiencing large dipolar interactions. In summary, for a heterogeneous system comprising

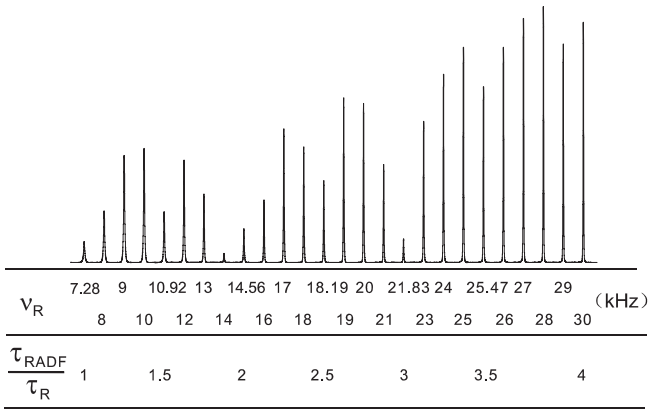

Fig. 4. RADF ^{1}H MAS spectra of the 1/1 GA mixture at $B_0 = 14.4$ T, versus MAS frequency. The RADF sequence (Fig. 1a) employs $\tau_p = 1.3$ μs and $\tau = 10.1$ μs, i.e. a cycle time $\tau_{RADF} = 12(\tau + \tau_p) = 136.8$ μs. The number of dipolar filter cycles is $M = 6$, which results in a total filter length of 821 μs. The MAS frequencies in kHz are indicated below the spectra. Integer and half-integer τ_{RADF}/T_R ratios, which results in destructive interferences between MAS and rf averaging, are indicated on the bottom of the figure. Whatever the MAS frequency, only the adamantane signals are visible in the RADF spectra.

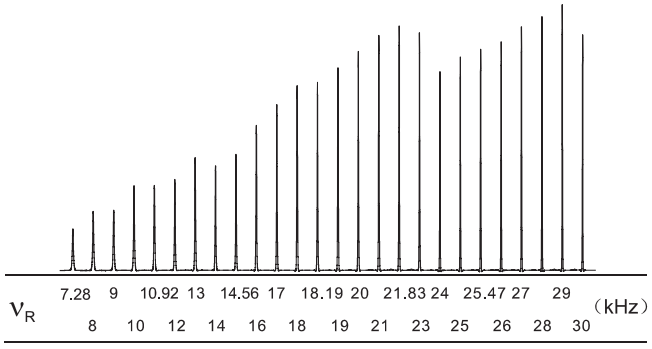

Fig. 5. RSDF ^{1}H MAS spectra of the 1/1 GA mixture at $B_0 = 14.4$ T, versus MAS frequency. For each MAS frequency, the integer n ($\neq 3$ k) was chosen, and the delay adjusted about $\tau \approx 12$ μs ($\tau_p = 2.6$ μs), in order for the RSDF cycle time $\tau_{RSDF} = 12(\tau + \tau_p)$ to be equal to nT_R, the cycle time of the $C6_n^3$ $(x, -x)$ sequence (Fig. 1b). The number M of repetition cycles was chosen so that the total filter length always remained around 0.8–1 ms. Whatever the MAS frequency, only the adamantane signals are visible in the RSDF spectra.

rigid and mobile segments, the RADF sequence suppresses the ^{1}H signal of rigid parts experiencing large ^{1}H–^{1}H dipolar interactions, but affects much less the signal of mobile segments.

However, the RADF sequence has been designed under static condition, and Magic-Angle Spinning (MAS) can interfere destructively with the rf-pulses [13]. Experimentally, the effectiveness of the RADF sequence is indeed largely reduced when the cycle time of the RADF pulse sequence, τ_{RADF}, is equal to an integer or half-integer number of rotor periods, T_R (see Fig. 4). These destructive interferences entail a careful adjustment of τ_{RADF} under MAS.

In this communication, we propose a Rotor-Synchronous Dipolar-Filter (RSDF) sequence (Fig. 1b), which avoids destructive interferences between MAS and rf-pulses and benefits from high resolution and high efficiency when the MAS frequency is larger than 12 kHz.

2. RSDF sequence

The design of a rotor-synchronized dipolar filter is facilitated by symmetry arguments [14,15]. In principle, all ^{1}H–^{1}H homo-nuclear CN_n^ν decoupling sequences can be employed for dipolar filtering.

For instance, we have recently shown that in the first-order AH, some CN_n^ν sequences suppress the terms arising from the ^1H–^1H dipolar interaction and the ^1H chemical shift anisotropy (CSA_H), while the isotropic chemical shift and hetero-nuclear J-coupling terms can be described as an effective field along the z-axis [16,17]. In the case of an I_2S spin system, with a suitable CN_n^ν dipolar filter on the I channel, the first-order AH can be written [14]:

$$\overline{H}^{(1)} = \kappa_{0010}^{C}\left(\Omega_{I1}^{0} I_{1z} + \Omega_{I2}^{0} I_{2z} + 2\pi J_{I1S} I_{1z} S_z + 2\pi J_{I2S} I_{2z} S_z\right) + 2\pi J_{I1I2} \boldsymbol{I}_1 \boldsymbol{I}_2 + \Omega_S^0 S_z \quad (1)$$

where Ω_{Ii}^0 and J_{IiS} denote respectively the isotropic chemical shift and hetero-nuclear J-coupling of I spins ($i = 1,2$), J_{I1I2} the homo-nuclear J-coupling and Ω_S^0 the isotropic chemical shift of S spin. The calculation of the κ_{0010}^C scaling factor [14] is not required here since this value does not affect the efficiency of the dipolar filter. The cycle time of the CN_n^ν sequence is equal to n rotor periods (T_R).

In this article, we focus on $C6_n^3$ symmetries with $n \neq 3k$, where k is an integer. These symmetries produce a first-order AH identical to that of Eq. (1). Conversely, $C6_{3k}^3$ symmetries reintroduce the ^1H–^1H dipolar interaction and the CSA_H and hence cannot be used as dipolar filter.

As long as the AH can be approximated with its first-order term, which means that the magnitudes of ^1H–^1H dipolar couplings are small compared to $1/(nT_R)$, the ^1H longitudinal magnetization only evolves under the effect of the J_{H-H} scalar couplings during the $C6_n^3$ sequences since the ^1H longitudinal magnetization is not affected by isotropic chemical shifts and hetero-nuclear J-couplings, which are along the z axis (see Eq. (1)). The evolution under J_{H-H} coupling during $C6_n^3$ sequences is not observed when the J-coupled ^1H sites display unresolved NMR signals, since the J-coupling term commutes with the total angular momentum operators along z axis. For instance, in the case of an I_2S spin system, we have $[I_{1z} + I_{2z}, \boldsymbol{I}_1\boldsymbol{I}_2] = 0$.

Conversely, when the magnitudes of ^1H–^1H dipolar couplings are large compared to $1/(nT_R)$, the first-order AH is not sufficient to describe the spin dynamics and additional higher-order terms must be taken into account. In this case, the ^1H longitudinal magnetization decays under the influence of ^1H–^1H dipolar-couplings, which are not canceled in these higher-order terms.

In this article, we employ as basic element $C = 90_0$-τ–90_{180}-τ in $C6_n^3$ sequences. Here 90_0 and 90_{180} denote rectangular, resonant rf pulses of length τ_p with flip angle 90° and phases 0° and 180° respectively, while τ is a window delay during which the rf-field is turned off. This basic element benefits from low rf-field requirement compatible with high MAS frequencies. Another example of windowed CN_n^ν basic element can be found in Eq. (76) of Brinkmann and Eden [14b]. For the sake of brevity, the $C6_n^3$ (90_0-τ–90_{180}-τ) sequences will be denoted RSDF in the following. For these sequences, the cycle time is $\tau_{RSDF} = nT_R = 12(\tau + \tau_p)$ and the corresponding pulse sequence is depicted in Fig. 1b.

Usually, the ^1H–^1H dipolar broadening for rigid segments is about 25–30 kHz and the peak width of the static ^1H spectra can reach up to 125 kHz. Therefore, the pulse length τ_p must be small (*e.g.* $\tau_p = 2$ μs with $\nu_{1H} = 125$ kHz) in order to excite uniformly the proton spectrum of the rigid segments. Furthermore, in order to relax the rigid segment signals efficiently, the delay τ should be larger than the inverse of the dipolar broadening for the rigid segments (e.g. $\tau = 8$–12 μs). These two factors lead to large n values since $n = 12(\tau + \tau_p)/T_R$. As an example, at $\nu_R = 30$ kHz and with $\tau \approx 12$ μs and $\tau_p = 2$ μs, it is easy to show that n should be equal to 5. The total length of dipolar filter $\tau_{tot} = nMT_R$ must be increased until the NMR signal of rigid segments is eliminated. More details about the optimization of RSDF sequence are given in the Supporting Information (Fig. S1).

3. Simulation of the dipolar-filtering efficiency of RSDF

At first, we demonstrate *in-silico* the filter efficiency of RSDF sequence at fast MAS, $\nu_R = 30$ kHz, with different repetition cycles M, without considering the incoherent decay processes. The simulations were performed using SIMPSON software (version 1.1.0) [18]. The powder averaging was accomplished using 2816 orientations: 256 {α_{MR}, β_{MR}}-pairs×11 γ_{MR}- angles. The 256 {α_{MR}, β_{MR}}-pairs, which relate the molecular and rotor frames, were selected according to the REPULSION algorithm [19]. All simulations presented here have been calculated on a H1–H2–H3 three-spin system, with dipolar coupling constants equal to $b_{H1-H2}/(2\pi) = -12$ kHz and $b_{H1-H3}/(2\pi) = b_{H2-H3}/(2\pi) = -2$ kHz, and isotropic chemical shifts equal to $\Omega_{H2}^0/(2\pi) = -\Omega_{H1}^0/(2\pi) = 9$ kHz and $\Omega_{H3}^0/(2\pi) = 1.5$ kHz. The CSA_H of the three protons as well as their J_{H-H} couplings were neglected. Interestingly, even in the absence of incoherent decay, Fig. 2 shows that the RSDF sequence effectively reduces the signals of the H1 and H2 sites experiencing large dipolar couplings, while the H3 intensity remains unaffected since $|b_{H1-H3}/(2\pi)| = |b_{H2-H3}/(2\pi)| < 1/\tau_{RSDF}$ and $|b_{H1-H2}/(2\pi)| > 1/\tau_{RSDF}$. This RSDF filtering effect, which has never been demonstrated before, is enhanced by incoherent decay processes and leads to a very effective elimination of the signal of the rigid components.

4. Samples and experimental conditions

The filtering efficiencies of the RADF and RSDF sequences were compared on a mixture of α-glycine and adamantane. These protonated solids are submitted to strong and weak ^1H–^1H dipolar couplings, respectively. The mixture we used, hereinafter referred to as GA, had a ^1H molar ratio of 1/1 or 2/1 in Figs. 3–5 and 7, respectively. Both samples were purchased from Aldrich-Sigma Corp. and used without any further treatment.

A three-block copolymer PCL/MDI/BDO (PCL: poly-caprolactone, MDI: 4,4'- di-phenyl-methane di-isocyanate and BDO: 1,4-butanediol) was also investigated. The samples of segmented polyurethanes were prepared by a two steps method involving end-capping appropriate quantities –OH terminated PCL with *liquid*

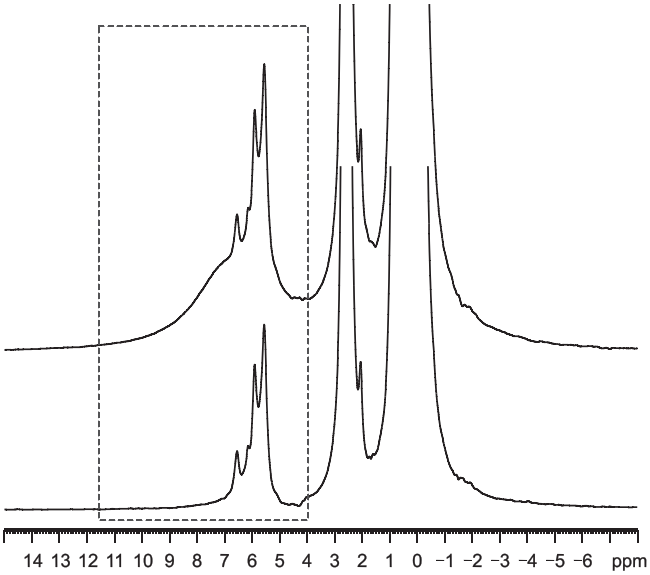

Fig. 6. The ^1H single pulse (above) and RSDF (below) MAS spectra of the three-block copolymer PCL/MDI/BDO at $\nu_R = 30$ kHz and $B_0 = 14.4$ T. The pulse and window lengths are $\tau = 11.3$ μs and $\tau_p = 2.6$ μs, respectively (Fig. 1b). The n and M values are 5 and 6, respectively, i.e. $\tau_{tot} = 1$ ms. The spectra are clipped in order to emphasize the dipolar filter effect.

MDI followed by the reaction with the *liquid* chain extender BDO in solution [20].

NMR experiments of Figs. 3–6 were performed at 14.4 T on a Bruker AVANCE-III spectrometer, with ^{1}H frequency of 600 MHz, and a commercial Bruker triple-resonance 2.5 mm probe, which allows spinning frequencies up to 35 kHz. NMR experiment of Fig. 7 and Fig. S1-3, were performed at 18.8 T on a Bruker AVANCE-III spectrometer, with ^{1}H frequency of 800 MHz, and a commercial Bruker triple-resonance 1.3 mm probe, which allows spinning frequencies up to 70 kHz. All experiments were carried out at room temperature and processed with Bruker Topspin 2.0 software. Each spectrum was accumulated with 8 scans separated with a recycling delay of 8 s.

5. RADF and RSDF experiments at MAS frequency below 30 kHz

Fig. 3 represents the 1/1 GA MAS spectrum versus spinning speed. With the increase of the MAS speed, the glycine resonance, which is very broad below $\nu_R \leqslant 10$ kHz, becomes observable, and the adamantane resonance narrows, thus leading to larger signal amplitude. The comparison between Figs. 3 and 4 shows the filtering effect of RADF sequence, as the broad glycine component is nearly not observable in Fig. 4, whatever the spinning speed. However, the destructive interference between MAS speed and RADF cycle-time can be observed through the dips in intensity displayed in Fig. 4. In principle, the effectiveness of the RADF sequence is strongly reduced, or even canceled out, if the ratio between the cycle-time and the rotor period, τ_{RADF}/τ_R, is equal to an integer or a half-integer number, since these destructive conditions recouple ^{1}H–^{1}H dipolar interactions and CSA_H. At ultra-fast MAS, e.g. $\nu_R = 80$ kHz [21], the dips should occur every 6 μs change for τ_{RADF} value, and this may lead to poor efficiency, especially when taking into account the spinning speed fluctuations which are not negligible with so small rotors. These interferences between MAS frequency and cycle time can also be observed in PMLG [22], DUMBO [23], and TIMES [24,25] sequences.

The dipolar filtering effect of RSDF can be observed in Fig. 5, which shows no interference with the spinning speed. By comparing Figs. 4 and 5, we can thus conclude that the RSDF sequence is the better choice at fast or ultra-fast MAS: $\nu_R > 12$ kHz. Indeed, the RADF sequence has been originally designed for static and quasi-static cases, and hence it performs well at slow MAS speed: $\nu_R < 12$ kHz. It should be pointed out that RSDF has a trace residue of glycine, because the same dipolar filter time as RADF is used here and partial recoupling of ^{1}H homo-nuclear coupling of RADF would better suppress the glycine signal. To fully eliminate the glycine residue, longer dipolar filter time ~1.4 ms can be used for RSDF.

The efficiency of RSDF sequence was also investigated in the case of three-block copolymer PCL/MDI/BDO. This copolymer comprises a rigid MDI segment, which is composed of benzene rings, and two soft PCL and BDO segments with the molar ratio of 1:4:3, respectively. The rigid MDI segment is obviously eliminated by RSDF sequence in Fig. 6, while the other two components are kept.

6. Experimental demonstration of RSDF filtering at ultra-fast MAS $\nu_R = 60$ kHz

Fig. 7 represents the effect of the total dephasing time, τ_{tot}, when the RSDF sequence is used at ultra-fast MAS with $\nu_R = 60$ kHz. It is interesting to note that the CH_2 group in glycine is quickly dephased with $\tau_{tot} \geqslant 0.8$ ms, while the NH_3 group is attenuated more slowly. However, the NH_3 group is almost eliminated at $\nu_R = 30$ kHz with the same dephasing time of $\tau_{tot} = 0.8$ ms (Fig. 5). At ultra-fast MAS, the effective attenuation of NH_3 group needs a much longer dephasing time of $\tau_{tot} \geqslant 4$ ms. This behavior suggests that the NH_3 group is detached from the proton bath at $\nu_R = 60$ kHz and rotates independently around its tetrahedral axis, which leads to a smaller dipolar coupling constant. The fact that the MAS spectrum of glycine gets fully resolved at this speed also indicates that its proton bath is broken and that it loses a part of its homogeneous characteristic, which means smaller homo-nuclear dipolar coupling constants. Another factor is that at ultra-fast MAS the coherence lifetimes are increased. At last it should be pointed out that the temperature rises from 30 °C to 50 °C when the spinning speed increases from 30 to 60 kHz, thus leading to more mobility of two species. More details about dipolar filtering at ultra-fast MAS are given in Fig. S2,3.

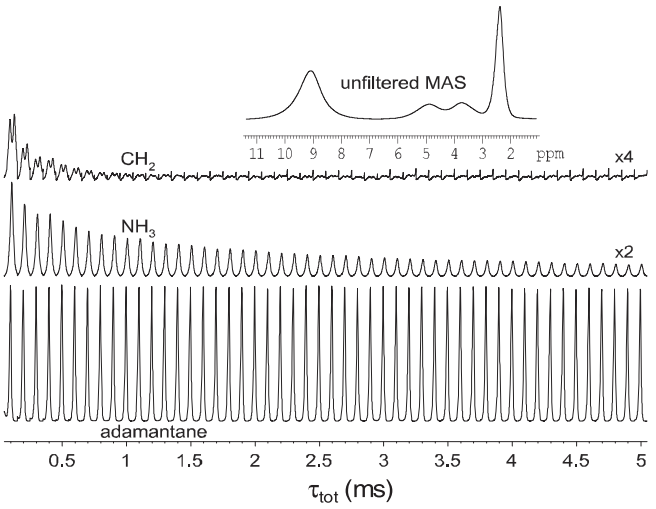

Fig. 7. Evolution of RSDF ^{1}H MAS spectra of the 2/1 GA mixture at $\nu_R = 60$ kHz and $B_0 = 18.8$ T as function of τ_{tot}. The pulse and window lengths are $\tau_p = 1.13$ μs and $\tau = 8.6$ μs, respectively, and $n = 7$. The CH_2 and NH_3 signal intensities of glycine are multiplied by a factor of 4 and 2, compared to that of adamantane. The intensities of glycine signals decrease with increasing τ_{tot}, while that of adamantane remains unaffected. Top: unfiltered MAS spectrum of the mixture allowing the evaluation of initial relative concentration and RSDF efficiency.

7. Conclusion

In this work, a new dipolar filter pulse sequence, called RSDF, has been proposed, which has the advantage of being rotor-synchronized, thus leading to a very simple experimental set up with a single parameter to be optimized. Therefore, compared to RADF sequence, RSDF does not suffer from destructive interferences between rf and MAS averaging. Furthermore, the RSDF sequence is more compatible with high MAS frequencies, while RADF can be a good choice in static and quasi-static condition (i.e. $\nu_R < 12$ kHz). Consequently RSDF complements the RADF sequence and it should be used for characterizing heterogeneous systems where high MAS frequencies are mandatory in order to record high-resolution proton 1D or 2D DQ–SQ spectra [26]. It should be interesting to probe the spin diffusion coefficient at fast or ultra-fast MAS with this new dipolar filter sequence [27]. It should be also interesting to study the "intra-molecular" NOE effect in systems exhibiting weak mobility contrast: a RSDF filter can be used to select the mobile side-group of a stiff-chain polymer and NOE effects instead of spin diffusion will lead to polarization re-equilibration [1b,28]. All these studies are in progress.

Acknowledgments

Authors are grateful for funding provided by Region Nord/Pas de Calais, Europe (FEDER), CNRS, French Minister of Science, USTL,

ENSCL, Contract No. ANR-2010-JCJC-0811-01 CortecNet and Bruker BIOSPIN. Financial support from the FR-3050 for conducting the research is gratefully acknowledged. Q. Liu is grateful for "ECNU Graduate Studies Research Program CX2011015". B. Hu is grateful for the funding supported by "the Fundamental Research Funds for the Central Universities". Q. Chen is grateful for "National fundamental research program 2007CB925200 and Shanghai Leading Talent Training Program".

Appendix A. Supplementary data

Supplementary data associated with this article can be found, in the online version, at doi:10.1016/j.jmr.2011.07.025.

References

[1] (a) F. Mellinger, M. Wilhem, H.W. Spiess, Calibration of ^{1}H NMR spin diffusion coefficients for mobile polymers through transverse relaxation measurements, Macromolecules 32 (1999) 4686–4691;
(b) M. Gaborieau, R. Graf, H.W. Spiess, Versatility of the dipolar-filter selection: from ^{1}H nuclear spin diffusion experiment to the measurement of nuclear overhauser effect in homo-polymer melts, Solid State Nucl. Mag. Reson. 28 (2005) 160–172.
[2] X. Wang, F. Tao, P. Sun, D. Zhou, Z. Wang, Q. Gu, J. Hu, G. Xue, Probing chain inter-penetration in polymer glasses by ^{1}H dipolar-filter solid-state NMR under fast magic angle spinning, Macromolecules 40 (2007) 4736–4739.
[3] M. Goldman, L. Shen, Spin–spin relaxation in LaF_3, Phys. Rev. 144 (1966) 321–331.
[4] D.L. VanderHart, Proton spin diffusion as a tool for characterizing polymer blends, Makromol. Chem., Macromol. Symp. 34 (1990) 125–159.
[5] K.J. Packer, J.M. Pope, The distortion of NMR spectra by multiple quantum coherence effects resulting from Goldman–Shen and related pulse sequences applied to heterogeneous solids, J. Magn. Reson. 55 (1983) 378–385.
[6] D.E. Demco, A. Johansson, J. Tegenfeldt, Proton spin diffusion for spatial heterogeneity and morphology investigations of polymers, Solid State Nucl. Magn. Reson. 4 (1995) 13–38.
[7] N. Egger, K. Schmidt-Rohr, B. Blümich, W.D. Domke, B. Stapp, Solid state NMR investigation of cationic polymerized epoxy resins, J. Appl. Polym. Sci. 44 (1992).
[8] J. Clauss, K. Schmidt-Rohr, H.W. Spiess, Determination of domain sizes in heterogeneous polymers by solid-state NMR, Acta Polym. 44 (1993) 1–17.
[9] D.L. VanderHart, G.B. McFaden, Some perspectives on the interpretation of proton NMR spin diffusion data in terms of polymer morphologies, Solid State Nucl. Magn. Reson. 7 (1996) 45–66.
[10] M. Antonietti, D. Radloff, U. Wiesner, H.W. Spiess, Structure and dynamics of polyelectrolyte-surfactant complexes as revealed by solid state NMR, Macromol. Chem. Phys. 197 (1996) 2713–2727.
[11] L.N. Huang, P. Karthik, P. Apkarian, R. Chaikof, L. Elliot, Engineered collagen–PEO nanofibers and fabrics, J. Biomater. Sci., Polym. Ed. 12 (2001) 979–993.
[12] P.F.W. Simon, R. Ulich, H.W. Spiess, U. Wiesner, Block copolymer-ceramic hybrid materials from organically modified ceramic precursors, Chem. Mater. 13 (2001) 3464–3486.
[13] X. Wang, Q. Gu, Q. Sun, D. Zhou, P. Sun, G. Xue, Characterization of polymer compatibility by ^{1}H dipolar-filter solid-state NMR under fast magic angle spinning, Macromolecules 40 (2007) 9018–9025.
[14] (a) A. Brinkmann, M.H. Levitt, Symmetry principles in the nuclear magnetic resonance of spinning solids: heteronuclear recoupling by generalized Hartmann–Hahn sequences, J. Chem. Phys. 115 (2001) 357–384;
(b) A. Brinkmann, M. Eden, Second order average Hamiltonian theory of symmetry-based pulse schemes in the nuclear magnetic resonance of rotating solids: application to triple-quantum dipolar recoupling, J. Chem. Phys. 120 (2004) 11726–11745.
[15] Y. Nishiyama, T. Yamazaki, T. Terao, Development of modulated rf sequences for decoupling and recoupling of nuclear-spin interactions in sample-spinning solid-state NMR: application to chemical-shift anisotropy determination, J. Chem. Phys. 124 (2006) 064304.
[16] J.P. Amoureux, B. Hu, J. Trébosc, Enhanced resolution in proton solid-state NMR with very-fast MAS experiments, J. Magn. Reson. 193 (2008) 305–307.
[17] O. Lafon, Q. Wang, B. Hu, J. Trébosc, F. Deng, J.P. Amoureux, Proton–proton homonuclear dipolar decoupling in solid-state NMR using rotor-synchronized *z*-rotation pulse sequence, J. Chem. Phys. 130 (2009) 014504.
[18] M. Bak, J.T. Rasmussen, N.C. Nielsen, SIMPSON: a general simulation program for solid-state NMR spectroscopy, J. Magn. Reson. 147 (2000) 296–330.
[19] M. Bak, N.C. Nielsen, REPULSION: a novel approach to efficient powder averaging in solid-state NMR, J. Magn. Reson. 125 (1997) 132–139.
[20] F. Li, X. Zhang, J. Hou, M. Xu, X. Luo, D. Ma, B.K. Kim, Studies on thermally stimulated shape memory effect of segmented polyurethanes, J. Appl. Polym. Sci. 64 (1997) 1511–1516.
[21] Y. Nishiyama, Y. Endo, T. Nemoto, H. Utsumi, K. Yamauchi, K. Hioka, T. Asakura, Very fast magic angle spinning ^{1}H-^{14}N 2D solid-state NMR: sub-micro-liter sample data collection in a few minutes, J. Magn. Reson. 208 (2011) 44–48.
[22] E. Vinogradov, P.K. Madhu, S. Vega, A bimodal Floquet analysis of phase modulated Lee–Goldburg high resolution proton magic angle spinning NMR experiments, Chem. Phys. Lett. 329 (2000) 207–214.
[23] A. Lesage, D. Sakellariou, S. Hediger, B. Elena, P. Charmont, L. Emsley, Experimental aspects of proton NMR spectroscopy in solids using phase-modulated homonuclear dipolar decoupling, J. Magn. Reson. 163 (2003) 105–113.
[24] Z. Gan, P.K. Madhu, J.P. Amoureux, J. Trébosc, O. Lafon, A tunable homonuclear dipolar decoupling scheme for high-resolution proton NMR of solids: from slow to fast magic-angle spinning, Chem. Phys. Lett. 503 (2011) 167–170.
[25] Y. Nishiyama, X. Lu, J. Trébosc, O. Lafon, Z. Gan, P.K. Madhu, J.P. Amoureux, A simple scheme for high-resolution ^{1}H solid-state NMR spectra at ultra-fast MAS and its application to ^{1}H-{^{13}C} *J*-HMQC experiments, J. Magn. Reson. Submitted.
[26] B. Hu, Q. Wang, O. Lafon, J. Trébosc, F. Deng, J.P. Amoureux, Robust and efficient spin-locked symmetry-based double-quantum homonuclear dipolar recoupling for probing ^{1}H-^{1}H proximity in the solid-state, J. Magn. Reson. 198 (2009) 41–48.
[27] (a) D. Reichert, T.J. Bonagamba, K. Schmidt-Rohr, Slow-down of ^{13}C spin diffusion in organic solids by fast MAS: a CODEX NMR study, J. Magn. Reson. 151 (2001) 129–135;
(b) Z. Jia, L. Zhang, Q. Chen, E.W. Hansen, Proton spin diffusion in polyethylene as a function of magic-angle spinning rate. A phenomenological approach, J. Phys. Chem. A 112 (2008) 1228–1233.
[28] (a) M. Gaborieau, R. Graf, S. Kahle, T. Pakula, H.W. Spiess, Chain dynamics in poly(n-alkyl acrylates) by solid-state NMR, dielectric and mechanical spectroscopies, Macromolecules 40 (2007) 6249–6256;
(b) M. Gaborieau, R. Graf, H.W. Spiess, Investigation of chain dynamics in poly(n-alkyl methacrylate)s by solid-state NMR: comparison with poly(n-alkyl acrylate)s, Macromol. Chem. Phys. 209 (2008) 2078–2086.